

# Inverse Design of Multilayer Broadband “RGBP” Freeform Metalens for Dual-Functional Color-sorting and Polarization Imaging

Pan, Cindy "Hsin"; Brand, Matthew

TR2025-055 May 10, 2025

## Abstract

We optimize an inverse-designed multilayer freeform dual-function metalens alternative to Bayer masks, achieving 60% color sorting and 51% polarization sorting efficiency—surpassing single-layer metalenses in both functions.

*Conference on Lasers and Electro-Optics (CLEO) 2025*

© 2025 MERL. This work may not be copied or reproduced in whole or in part for any commercial purpose. Permission to copy in whole or in part without payment of fee is granted for nonprofit educational and research purposes provided that all such whole or partial copies include the following: a notice that such copying is by permission of Mitsubishi Electric Research Laboratories, Inc.; an acknowledgment of the authors and individual contributions to the work; and all applicable portions of the copyright notice. Copying, reproduction, or republishing for any other purpose shall require a license with payment of fee to Mitsubishi Electric Research Laboratories, Inc. All rights reserved.



# Inverse Design of Multilayer Broadband “RGPB” Freeform Metalens for Dual-Functional Color-sorting and Polarization Imaging

Cindy (Hsin) Pan,<sup>1,2</sup> Matt Brand,<sup>1,\*</sup>

<sup>1</sup> Mitsubishi Electric Research Labs (MERL), 201 Broadway, Cambridge MA, USA

<sup>2</sup> Department of Electrical and Computer Engineering, Princeton University, Princeton NJ, USA

\*brand@merl.com

**Abstract:** We optimize an inverse-designed multilayer freeform dual-function metalens alternative to Bayer masks, achieving 60% color sorting and 51% polarization sorting efficiency—surpassing single-layer metalenses in both functions. © 2024 The Author(s)

## 1. Introduction

Traditional camera systems rely on Bayer color filters and polarizing filters for image reconstruction, limiting energy utilization efficiency and sensitivity. To overcome these constraints, metalens-integrated camera sensor systems incorporate sub-wavelength structures that reshape wavefronts, enabling enhanced image quality in low-light conditions [1, 2]. We present an inverse-designed multilayer freeform dual-functional metalens using FDTD and adjoint optimization for full-color imaging and polarization sorting, achieving 60% average color sorting efficiency and 51% polarization sorting efficiency, outperforming the existing single layer color sorting metalenses while simultaneously demonstrating effective polarization sorting capabilities.

## 2. Inverse Design

Freeform multilayer metalens inverse design is accomplished through topology optimization, utilizing adjoint-based methods within MEEP simulator [5]. Each metalens unit cell measures  $3.2\ \mu\text{m}$  by  $3.2\ \mu\text{m}$ , featuring a  $0.5\ \mu\text{m}$  thick  $\text{SiO}_2$  substrate and  $SN$  nanopillars with height of  $0.7\ \mu\text{m}$ . Optimization is achieved through an iterative loop that integrates the NLOpt algorithm with the FDTD solver. Periodic boundary conditions were applied along the metalens plane, with perfectly matched layer (PML) boundaries in the propagation direction, and the simulation covered the visible range. As shown in Fig. 1a. and Fig. 1c., the initial design phase began by defining four distinct target phase profiles, each centered in a quadrant of the unit cell to match an RGGGB Bayer arrangement.

A library was used to map subwavelength nanopillar dimensions to corresponding phase shifts. The first layer’s initial design consist of nanopillar dimensions that minimize phase error across all four target profiles, while the second layer started with dummy nanopillars. Fig. 1d. shows the initial configuration, optimizing the phase distribution and providing a solid starting point for optimization. In Fig. 1b., forward simulation evaluates focal plane intensity and checks for convergence. Adjoint optimization then computes gradients to update design parameters. Target focal plane intensity is achieved through iterative forward simulation and gradient-based optimization. Full-color imaging was demonstrated with a virtual metalens-integrated camera sensor system. Fig. 1e. shows the experimental setup with an imaging lens positioned three focal distances from the scene and the metalens array placed  $75\ \text{mm}$  from the imaging lens. The image sensor pairs with the metalens array, a 2D periodic Bayer cell with optimized design weights at a focal distance of  $f = 4\ \mu\text{m}$ . After 360 optimization iterations, the final Bayer cell with optimized freeform nanopillars in both layers is shown in Fig. 1f.

We evaluated performance by virtually measuring the focal plane intensity of a single pixel under collimated white beam illumination. Fig. 1g. shows the pixel’s focal plane intensity distributions under horizontally polarized light (top), vertically polarized light (middle), and unpolarized white light (bottom). The color sorting performance of the proposed and baseline metalenses was evaluated by color sorting efficiency, the ratio of power collected in each color quadrant to the total incident power on the unit cell for a given wavelength. Table 1 summarizes a comparison of these efficiencies. The color sorting efficiencies at  $635\ \text{nm}$  (red),  $520\ \text{nm}$  (green), and  $430\ \text{nm}$  (blue) are 55%, 72%, and 52%, respectively, significantly outperforming baseline approaches [1, 2]. Polarization sorting efficiency is defined as the ratio of correctly sorted polarized light power to the total incident power on the unit cell for a given wavelength. The average polarization sorting efficiency of the proposed metalens is 51%, which is comparable to that of the leading polarization imaging metalenses [3, 4]. We evaluated imaging performance across the visible spectrum by using sample scenes and measuring each pixel’s Bayer spectral response with our metalens

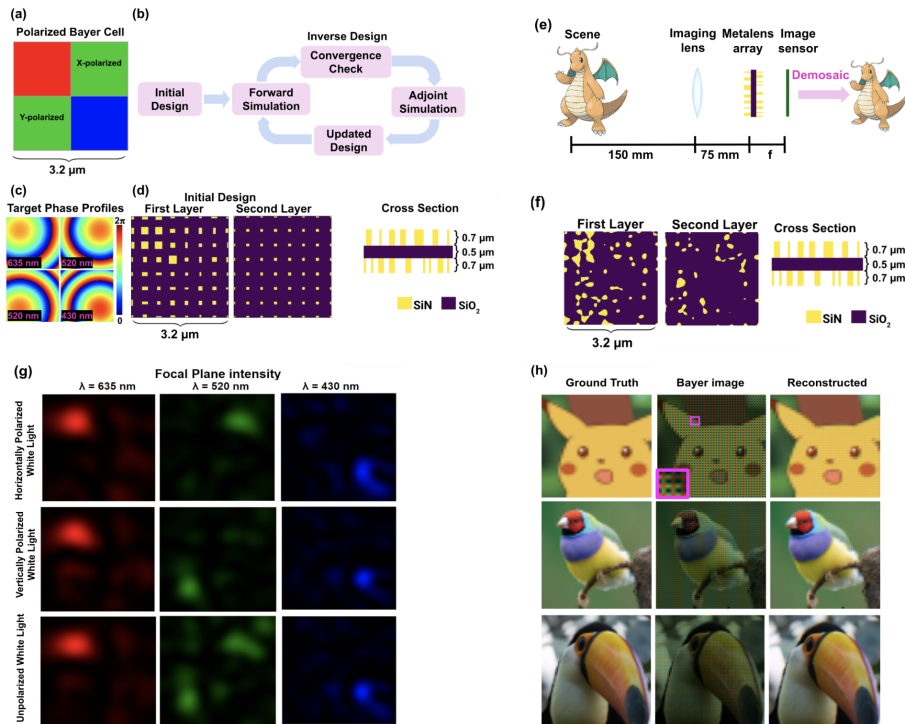


Fig. 1. (a) Target Bayer cell: incident light is sorted and focused into four color-specific finite-difference time-domain pixels, with the two green pixels focusing horizontally and vertically polarized light. (b) Inverse design flowchart. (c) Target phase profiles for red, green, and blue. (d) Initial design and its cross-section view. (e) Color imaging experimental Setup. (f) Optimized Bayer cell structure. (g) Focal plane intensity at 635 nm, 520 nm, and 430 nm for a pixel illuminated by horizontally polarized, vertically polarized, and unpolarized white light. (h) Full-color imaging: the left column shows ground truth images, the middle shows RRGB Bayer images by spectral response, and the right shows reconstructed images.

array. The image sensor then captured a raw grayscale mosaic, with each pixel corresponding to a single Bayer cell. To reconstruct three-channel color image from the grayscale RRGB Bayer image, standard demosaicing interpolation is applied. Fig. 1h. shows the ground truth images, RRGB Bayer images, and reconstructed images, demonstrating the high-fidelity color reconstruction of our proposed metalens array.

Table 1. Comparison with Baseline Methods

	Red	Green	Blue	Average Color Sorting Efficiency	Average Polarization Sorting Efficiency	Numerical Aperture
Zou et al [1]	58%	59%	49%	55%	N/A	0.19
Miyata et al [2]	65%	50%	25%	47%	N/A	0.2
<b>Proposed</b>	<b>55%</b>	<b>72%</b>	<b>52%</b>	<b>60%</b>	<b>51%</b>	<b>0.4</b>

In summary, we demonstrated a visible-range multilayer freeform metalens for full-color imaging and polarization sorting, with the freeform structure and second layer provide additional degrees of freedom for optimization. Our simulation results validated the optimized design, showing superior color sorting efficiency over baseline methods and effective polarization sorting comparable to leading metalenses.

## References

1. Zou, X., Zhang, Y., Lin, R. et al. Nat. Commun. 13, 3288 (2022). <https://doi.org/10.1038/s41467-022-31019-7>.
2. Miyata, M., Nemoto, N., Shikama, K., Kobayashi, F., & Hashimoto, T. Optica 8, 1596-1604 (2021).
3. Shen, S., Li, S., Yuan, Y., & Tan, H. Opt. Express 31, 28611-28623 (2023).
4. Sun, X., Ma, R., Pu, X., Ge, S., Cheng, J., Li, X., Wang, Q., Zhou, S., & Liu, W. Nanomaterials 12(9), 1500 (2022). doi: 10.3390/nano12091500.
5. Oskooi, A. F., Roundy, D., Ibanescu, M., Bermel, P., Joannopoulos, J. D., & Johnson, S. G. Comput. Phys. Commun. 181(3), 687-702 (2010).